
Reliability analysis and matpower simulation of IEEE14 node based on mixed entropy measure

Zhenhua Shao^{1,2,3,*}, Zhixiong Zhong^{1,2,3}, Wenzhong Lin^{1,2,3}

1. China Digital Fujian IoT Laboratory of Intelligent Production
Minjiang University, Fujian 350108, China
2. Fujian Province Key Laboratory of Information Processing and Intelligent Control
Minjiang University, Fujian 350108, China
3. College of Computer and Control Engineering, Minjiang University,
Fujian 350108, China
172097792@qq.com

ABSTRACT. With the increasingly large-scale interconnection of power system, the object of this paper was to analyze the fragility of the fault of IEEE14 nodes based on the mixed entropy measure. The mixed entropy approach was adopted to quantify the fragile links in the system, which is made up by the flow entropy and the risk entropy. The simulation experiments involved in the study were implemented in the MATPOWER toolbox of the MATLAB platform. The results obtained in this study include that the flow entropy is the key factor on unbalanced distribution of power grid, furthermore the safety of the whole power grid can be achieved a quantitative assessment by the risk entropy. The simulation experiments of IEEE-14 node involved in the study were implemented in the MATPOWER toolbox of the MATLAB platform. The results were presented in the form of data and histograms. The impacts of the obtained results are that the transfer entropy is modified by distribution entropy of power flow. the findings of this study may do good to the power network vulnerability analysis with large nodes.

RÉSUMÉ. Avec l'interconnexion de plus en plus large du système électrique, l'objet de cet article était d'analyser la fragilité de la défaillance des nœuds IEEE14 basé sur la mesure d'entropie mixte. L'approche d'entropie mixte a été adoptée pour quantifier les liens fragiles dans le système, constitués de l'entropie du flux et de l'entropie du risque. Les expérimentations de simulation engagées dans l'étude ont été mises en œuvre dans la boîte à outils MATPOWER de la plate-forme MATLAB. Les résultats obtenus dans cette étude indiquent que l'entropie du flux est le facteur clé de la répartition déséquilibrée du réseau électrique. De plus, la sécurité de l'ensemble du réseau électrique peut être réalisée à une évaluation quantitative par l'entropie du risque. Les expérimentations de simulation du nœud IEEE-14 impliquées dans l'étude ont été mises en œuvre dans la boîte à outils MATPOWER de la plate-forme MATLAB. Les résultats ont été présentés sous forme de données et d'histogrammes. L'impact des résultats obtenus est que l'entropie de transfert est modifiée par l'entropie de distribution du flux de puissance. Les

résultats de cette étude pourraient être utiles à l'analyse de la vulnérabilité du réseau électrique avec de grands nœuds.

KEYWORDS: mixed entropy, chain failures, vulnerability, reliability analysis.

MOTS-CLÉS: entropie mixte, pannes de chaîne, vulnérabilité, analyse de fiabilité.

DOI:10.3166/EJEE.20.573-588 © 2018 Lavoisier

1. Introduction

Power systems are the large-scale interconnected systems consisting of subsystems with unknown parameters. Chained failures may cause large scale blackout and lead to serious consequences. Moreover, it is rather difficult to search the modes of chained failures and analyze the consequences. In order to deal with chained failures of power grid and reasonable and effective evaluation on power system reliability, many researchers pay much more attention on reliability analysis on power system or power network (Thomasian and Blaum, 2006; Creen *et al.*, 2003; Christopher *et al.*, 2014; Iacoboaiea *et al.*, 2016; Blažej and Juraj, 2014; Carvalho *et al.*, 2018). Furthermore, security-constrained power flow optima and redistribution of power flow plays an important role in the propagation of chain failures (Kazemdehdashti *et al.*, 2018; Wang *et al.*, 2018; Fang *et al.*, 2017; Barocio *et al.*, 2017).

There are a large number of studies on analysis on solving security-constrained optimal power flow (SCOPF) with the help of Monte Carlo simulation (Monticelli *et al.*, 1987; Stott *et al.*, 1987; Wood *et al.*, 2014; Momoh, 2009; Zhu, 2009). While the major shortcoming of random-gradient-based methods is that the power flow quantitative evaluation and the reliability analysis cannot be reached on small sample. Moreover, the list popular evolutionary algorithm methods (e.g. genetic algorithms, evolution strategies, differential evolution, artificial immunological systems, etc.) is not a global optimization method. The system stability and vulnerability analysis on power grid is influenced by the initial iteration value and the random-gradient direction (Shahidehpour *et al.*, 2002; Capitanescu, 2011; Capitanescu and Wehenkel, 2012). Conversely, the mixed entropy method will be introduced to cope with the power network vulnerability analysis with large nodes (Phan and Kalagnanam, 2012; Marano-Marcolini *et al.*, 2012; Wang *et al.*, 2013).

The basic idea for using mixed entropy method in network vulnerability analysis is the nonlinear combination of power flow entropy and risk entropy (Ardakani and Bouffard, 2013; Platbrood *et al.*, 2014; Wang *et al.*, 2018). On one hand, network risk entropy plays an important role in assessment on system symmetry and topological structure of the whole network. On the other hand, the power flow entropy is the combination of power flow transfer factor and power flow distribution factor. The former is connected with the branch outage, while the latter is connected with the chain failures. The difference between network risk entropy and power flow entropy is shown in Table 1. Finally, the proposed method of mixed entropy measure of IEEE-14 node involved in the study were implemented in the MATPOWER toolbox of the MATLAB platform. The results were presented in the form of data and histograms.

Table 1. Comparison between different entropy

Type of entropy	Power flow transfer factor	Power flow distribution factor	Risk entropy
Emphasis point	Potential fault with branch outage	Outage resistance	Uncertain of system outage
Advantage	Transfer connected with power flow	Chain failure connected with branch	Reliability analysis connected with unbalance grid
Disadvantage	Reliability analysis is ignored	Network unbalance is ignored	Power flow transfer is ignored

The reminder of this paper is organized as follows. Section 2 presents the methodology introduction for the mixed entropy measure. Section 3 describes the power flow fluctuation of load side and generation side. Simulation and analysis are studied in Section 4. The conclusions are drawn in Section 5.

2. Methodology

There are three subsections are made up in this Section. In the first one, the basic entropy theory is described. In the second subsection, the basic concept of IEEE 14 node framework is introduced. Finally, in the third subsection, load fluctuations under three different conditions are discussed.

2.1. Basic theory of entropy on power flow

The definition of entropy is:

$$H = -\sum_{i=1}^N I_i \ln I_i \tag{1}$$

2.1.1. Power flow entropy Q_E

Q_E is made up by power flow transfer factor Q_{Ti} and power flow distribution factor Q_{Di} . $Q_E = Q_{Ti} Q_{Di}$

$$\Delta P_{ji} = P_{ji} - P_{j0}, j \neq i \tag{2}$$

where ΔP_{ji} is transfer number of branch j to branch i, δ_{ji} is transfer impact rate, E_T is the power flow entropy factor.

$$\Delta P_{ia} = P_{ia} - P_{i0} \quad (3)$$

$$\Delta P_a = \sum_{i=1}^N (P_{ia} - P_{i0}) \quad (4)$$

$$\delta_{ia} = \frac{\Delta P_{ia}}{\Delta P_a} \quad (5)$$

$$E_{Dia} = -\delta_{ia} \ln \delta_{ia} \quad (6)$$

$$E_{Di} = E_{DiaG} - E_{DiaL} = \delta_{iaL} \ln \delta_{iaL} - \delta_{iaG} \ln \delta_{iaG} \quad (7)$$

$$Q_{Di} = \frac{1}{2} \frac{1}{N_G N_L} \sum_{a_G \in G} \sum_{a_i \in L} \{E_{Di} + \max E_{Di}\} \quad (8)$$

Where ΔP_{ia} is the increment of power flow, ΔP_a is the sum of the increment of power flow for node a, δ_{ia} is the distribution impact rate from node a to branch I, E_{Dia} is the power flow entropy between node a and branch I, E_{Di} is the sum distribution impact rate of branch I.

2.1.2. Power flow risk entropy H_R

The risk entropy H_R and V_R between branch j and branch i is defined as:

$$V_R = \frac{H_{Rj} - H_{\min}}{H_{\max} - H_{\min}} \quad (9)$$

$$\Delta P_{ij} = |P_{ij} - P_{i0}| \quad (10)$$

$$\Delta P_j = \sum_{i=1}^L |P_{ij} - P_{i0}| \quad (11)$$

$$\eta_{ij} = \frac{\Delta P_{ij}}{\Delta P_j} \quad (12)$$

$$H_{Rj} = -\sum_{i=1}^L \eta_{ij} \ln \eta_{ij} \quad (13)$$

where ΔP_{ij} is the real power variation between node j and branch I, ΔP_j is the total real power variation of node j, η_{ij} is the relative change rate between node j and node i, H_R is the risk entropy of node i, and V_R is the index for reliability analysis.

2.2. power flow calculation of IEEE 14

As is shown in Figure 1, the whole frame of IEEE14 system is made up by 5 generator bus (1,2,3,6,8) and 11 load nodes (2,3,4,5,6,9,10,11,12,13,14), and the active power and real power parameters are shown in table 2 and table 3.

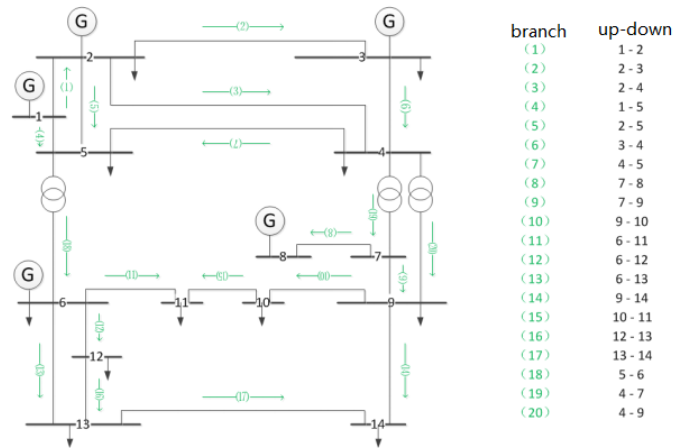


Figure 1. The whole frame of IEEE14 system

Table 2. Power flow calculation parameters of IEEE 14

Node Number	$P(MW)$	$Q(MVar)$	$S(MVA)$
Node 2	21.70	12.70	25.14
Node 3	94.20	19.00	96.10
Node 4	47.80	-3.90	47.96
Node 5	7.60	1.60	7.77
Node 6	11.20	7.50	13.48
Node 9	29.50	16.60	33.85
Node 10	9.00	5.80	10.71
Node 11	3.50	1.80	3.94
Node 12	6.10	1.60	6.31
Node 13	13.50	5.80	14.69
Node 14	14.90	5.00	15.72

Table 3. Upper limit active power value and real power value of generators

Generator number	P_{max}	P_{min}	Q_{max}	Q_{min}
Generator 1	332.4	0	10	0
Generator 2	140	0	50	-40
Generator 3	100	0	40	0
Generator 6	100	0	24	-6
Generator 8	100	0	24	-6

2.3. load fluctuation under three different conditions

In order to simplify the calculation process results, there are only three load fluctuation conditions considered in this paper. And the generators reactive power constraints are shown in Table 4. And the load fluctuations under different conditions are shown from Table 5 to Table 7. Condition A: the reactive power is increased and the real power is constant. Condition B: the real power is increased and the reactive power is constant. Condition C: the reactive power and the real power are increased in the same proportion.

Table 4. Reactive power constraints of generators

	generator1	generator2	generator3	generator6	generator8
NODE 2	-11.68*	47.55	25.04	12.72	17.61
NODE3	5.57	26.44	68.48*	12.61	17.40
NODE4	-2.85*	49.60	33.71	18.61	21.26
NODE5	-14.46*	43.88	25.59	13.45	17.86
NODE6	-15.16*	40.18	24.32	16.00	17.57
NODE9	-11.74*	36.09	23.63	18.32	20.22
NODE10	-15.22*	40.99	24.51	14.41	18.07
NODE11	-16.8*	42.52	24.85	13.75	17.72
NODE12	-15.78*	41.73	24.68	15.71	17.68
NODE13	-14.78*	39.54	24.19	17.88	17.73
NODE14	-14.32*	39.55	24.30	17.52	18.72
NODE WITH REACTIVE POWER	53.72*	33.09	75.69	49.15	27.30

Where * stands for reactive power constraints

Table 5. Load fluctuations under condition A

NODE NUMUBER	RESULTS	generator	load fluctuations factor
NODE2	bus2 P: 2.169630e+01 Q: 1.270000e+01 The generator of number 1 has violated Q constraints	1	(0~1]
NODE3	bus3 P: 9.420303e+01 Q: 19 The generator of number 1 has violated Q constraints	1	(0~1]
NODE4	bus4 P: 4.780117e+01 Q: -3.900000e+00 The generator of number 1 has violated Q constraints	1	(0~1]
NODE5	bus5 P: 7.603479e+00 Q: 600000e+00 The generator of number 1 has violated Q constraints	1	(0~1]
NODE6	bus6 P: 1.120091e+01 Q: 7.500000e+00 The generator of number 1 has violated Q constraints	1	(0~1]
NODE9	bus9 P: 2.950021e+01 Q: 1.660000e+01 The generator of number 1 has violated Q constraints	1	(0~1]
NODE10	bus10 P: 9.003560e+00 Q: 5.800000e+00 The generator of number 1 has violated Q constraints	1	(0~1]
NODE11	bus11 P: 33504797e+00 Q: 1.800000e+00 The generator of number 1 has violated Q constraints	1	(0~1]
NODE12	bus12 P:6.103778e+00 Q: 600000e+00 The generator of number 1 has violated Q constraints	1	(0~1]

NODE13	bus13 P: 1.349652e+01 Q: 5.800000e+00 The generator of number 1 has violated Q constraints	1	(0~1]
NODE14	bus14 P: 1.1490364e+01 Q: 5+00 The generator of number 1 has violated Q constraints	1	(0~1]

Table 6. Load fluctuations under condition B

NODE NUMUBER	RESULTS	generator	load fluctuations factor
NODE2	bus2 P: 2.17000e+01 Q: 270000e+01 The generator of number 1 has violated Q constraints	1	(0~1]
NODE3	bus3 P: 9.420000e+01 Q: 19 The generator of number 1 has violated Q constraints	1	(0~1]
NODE4	bus4 P: 4.780000e+01 Q: -3.900000e+00 The generator of number 1 has violated Q constraints	1	(0~1]
NODE5	bus5 P: 7.600000e+00 Q: 1.600000e+00 The generator of number 1 has violated Q constraints	1	(0~1]
NODE6	bus6 P: 1.120000e+01 Q: 7.500000e+00 The generator of number 1 has violated Q constraints	1	(0~1]
NODE9	bus9 P: 2.950000e+01 Q: 1.660000e+01 The generator of number 1 has violated Q constraints	1	(0~1]
NODE10	bus10 P: 9 Q: 5.800000e+00	1	(0~1]

	The generator of number 1 has violated Q constraints		
NODE11	bus11 P: 3.500000e+00 Q: 1.800000e+00 The generator of number 1 has violated Q constraints	1	(0~1]
NODE12	bus12 P: 6.100000e+00 Q: 1.600000e+00 The generator of number 1 has violated Q constraints	1	(0~1]
NODE13	bus13 P: 1.350000e+01 Q: 5.800000e+00 The generator of number 1 has violated Q constraints	1	(0~1]
NODE14	bus14 P: 1.490000e+01 Q: 5 The generator of number 1 has violated Q constraints	1	(0~1]

Table 7. Load fluctuations under condition C

NODE NUMUBER	RESULTS	generator	load fluctuations factor
NODE2	bus2 P: 2.170000e+01 Q: 1.270000e+01 The generator of number 1 has violated Q constraints	1	(0~1]
NODE3	bus3 P: 9.420000e+01 Q: 19 The generator of number 1 has violated Q constraints	1	(0~1]
NODE4	bus4 P: 4.780000e+01 Q: -3.900000e+00 The generator of number 1 has violated Q constraints	1	(0~1]
NODE5	bus5 P: 7.600000e+01 Q: 1.600000e+00 The generator of number 1 has violated Q constraints	1	(0~1]
NODE6	bus6 P: 1.120000e+01	1	(0~1]

	Q: 7.500000e+00 The generator of number 1 has violated Q constraints		
NODE9	bus9 P: 2.950000e+01 Q: 1.660000e+01 The generator of number 1 has violated Q constraints	1	(0~1]
NODE10	bus10 P: 9 Q: 5.800000e+00 The generator of number 1 has violated Q constraints	1	(0~1]
NODE11	bus11 P: 3.500000e+00 Q: 1.800000e+00 The generator of number 1 has violated Q constraints	1	(0~1]
NODE12	bus12 P: 6.100000e+01 Q: 1.600000e+00 The generator of number 1 has violated Q constraints	1	(0~1]
NODE13	bus13 P: 1.350000e+01 Q: 5.800000e+00 The generator of number 1 has violated Q constraints	1	(0~1]
NODE14	bus14 P: 1.490000e+01 Q: 5 The generator of number 1 has violated Q constraints	1	(0~1]

Compared table 3 with table 4 and table 5, we can draw a conclusion that the maximum load fluctuations factor is 1 under three different conditions. Otherwise, reactive power constraints of generators will be happened.

3. Mixed entropy of IEEE 14 network

In order to verify the efficiency of mixed entropy measure on IEEE14 network, the different set of experiments are carried out in the MATPOWER toolbox of the MATLAB platform. Moreover the flow charts of power flow transfer entropy and power flow distribution entropy are shown in Figure 2 and Figure 4. Moreover, the experiment results of two entropy methods under MATPOWER toolbox are shown in Figure 3 and Figure 5.

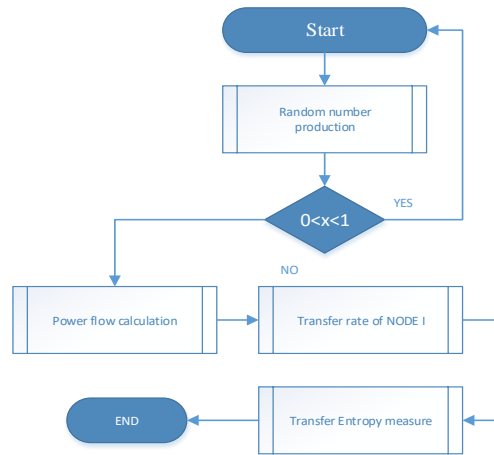


Figure 2. Flow chart of power flow transfer entropy

Compared with the Figure 3 and Figure 5, we can draw the conclusion that the permutation of transfer entropy and distribution entropy are shown in table 8-10. and the sequence of distribution entropy is shown in fig.6. which means that the node 2 is the vulnerabilities in the whole network. The first set is based on IEEE 14 BUS test system. For a comparison between the mixed entropy method and power flow entropy method (or risk entropy method), the different scheduling order are shown in Fig.6 and Fig.7. As can be seen from the Fig.6(mixed entropy method), the node 3,4,5 have the same risk entropy. However, we can only draw the conclusion that the node 2 is the vulnerabilities in the whole network.

Command Window									
4	2	4	56.38	-0.73	-54.68	2.26	1.692	5.13	
5	2	5	41.81	2.55	-40.89	-3.41	0.922	2.82	
6	3	4	-23.10	5.30	23.47	-5.66	0.374	0.95	
7	4	5	-60.68	17.99	61.20	-16.35	0.518	1.63	
8	4	7	28.04	-10.09	-28.04	11.81	0.000	1.72	
9	4	9	16.06	-0.60	-16.06	1.90	-0.000	1.31	
10	5	6	44.15	11.31	-44.15	-6.92	0.000	4.40	
11	6	11	7.39	3.70	-7.33	-3.58	0.057	0.12	
12	6	12	7.79	2.52	-7.72	-2.37	0.072	0.15	
13	6	13	17.77	7.29	-17.55	-6.87	0.213	0.42	
14	7	8	-0.00	-17.57	0.00	18.05	0.000	0.48	
15	7	9	28.04	5.75	-28.04	-4.95	0.000	0.80	
16	9	10	5.20	4.09	-5.18	-4.05	0.012	0.03	
17	9	14	9.40	3.52	-9.29	-3.28	0.115	0.24	
18	10	11	-3.82	-1.75	3.83	1.78	0.013	0.03	
19	12	13	1.62	0.77	-1.62	-0.76	0.006	0.01	
20	13	14	5.67	1.83	-5.61	-1.72	0.055	0.11	
Total:							13.241	54.05	

Figure 3. Experiment results of transfer entropy under MATPWOER

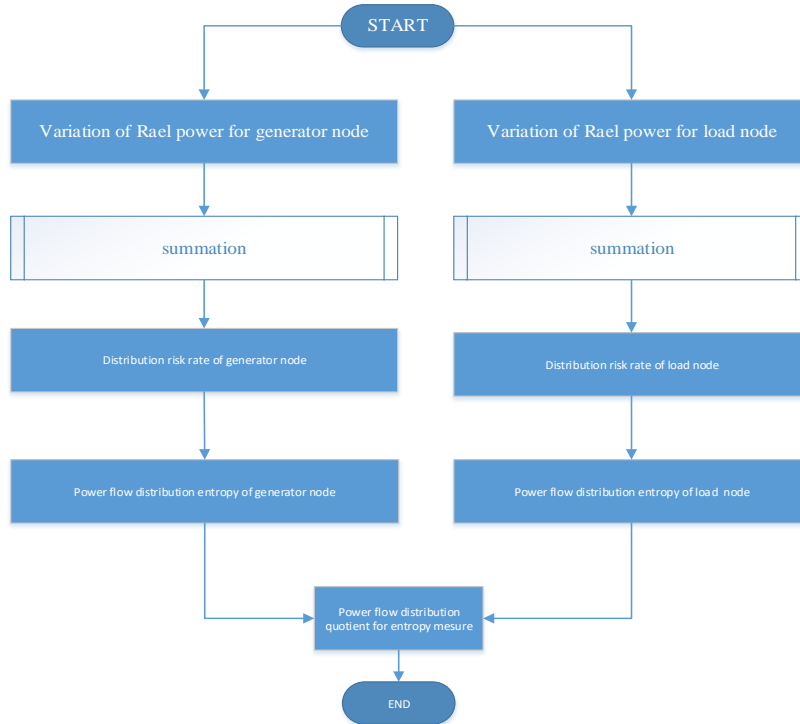


Figure 4. Flow chart of power flow of distribution entropy

Command Window								
4	2	4	55.50	-1.40	-53.86	2.76	1.639	4.97
5	2	5	40.66	1.42	-39.79	-2.45	0.868	2.65
6	3	4	-23.57	4.60	23.95	-4.94	0.383	0.98
7	4	5	-61.99	16.19	62.52	-14.53	0.529	1.67
8	4	7	28.04	-9.68	-28.04	11.38	0.000	1.70
9	4	9	16.06	-0.43	-16.06	1.73	0.000	1.30
10	5	6	44.14	12.46	-44.14	-8.02	0.000	4.43
11	6	11	7.39	3.55	-7.33	-3.44	0.056	0.12
12	6	12	7.79	2.50	-7.72	-2.35	0.072	0.15
13	6	13	17.77	7.21	-17.55	-6.79	0.212	0.42
14	7	8	-0.00	-17.17	0.00	17.63	-0.000	0.46
15	7	9	28.04	5.79	-28.04	-4.99	0.000	0.80
16	9	10	5.19	4.23	-5.18	-4.19	0.013	0.03
17	9	14	9.40	3.62	-9.29	-3.37	0.116	0.25
18	10	11	-3.82	-1.61	3.83	1.64	0.013	0.03
19	12	13	1.62	0.75	-1.61	-0.75	0.006	0.01
20	13	14	5.67	1.74	-5.61	-1.63	0.054	0.11
Total:							14.006	56.53

Figure 5. Experiment results of distribution entropy under MATPWOER

Table 8. Transfer entropy

number	test1	test2	test3	test4	test5	average
node2	1.298603	1.298620	1.298616	1.298626	1.298620	1.30
node3	1.929835	1.929849	1.929832	1.929824	1.929825	1.93
node4	2.112372	2.112372	2.112372	2.112372	2.112372	2.11
node5	1.828546	1.828548	1.828549	1.828547	1.828549	1.83
node6	2.633288	2.633288	2.633282	2.633289	2.633287	2.63
node9	2.739682	2.739690	2.739687	2.739690	2.739692	2.74
node10	2.683222	2.683221	2.683219	2.683225	2.683216	2.68
node11	2.532113	2.532119	2.532114	2.532116	2.532116	2.53
node12	2.742392	2.742389	2.742391	2.742390	2.742389	2.74
node13	2.716629	2.716629	2.716629	2.716629	2.716629	2.72
node14	2.698687	2.698684	2.698684	2.698688	2.698687	2.70

Table 9. Distribution entropy

Number	test1	test2	test3	test4	test5	average
node2	-0.09355856	-0.08894123	-0.07713753	-0.1428928	-0.1347842	-0.11
node3	-0.6137061	-0.6127401	-0.6151092	-0.6107501	-0.6131079	-0.61
node4	-0.7826699	-0.7856685	-0.7851088	-0.7717788	-0.7743651	-0.78
node5	-0.7570722	-0.7396852	-0.7577844	-0.7399870	-0.7579246	-0.75
node6	-1.335513	-1.339591	-1.340334	-1.331429	-1.333509	-1.34
node9	-1.432500	-1.433163	-1.430637	-1.427934	-1.431422	-1.43
node10	-1.365670	-1.350894	-1.350821	-1.362479	-1.354593	-1.36
node11	-1.285974	-1.295250	-1.287376	-1.291148	-1.291902	-1.29
node12	-1.444787	-1.446974	-1.448250	-1.449639	-1.451017	-1.45
node13	-1.426913	-1.423656	-1.421644	-1.422398	-1.426396	-1.42
node14	-1.384793	-1.392451	-1.390621	-1.388106	-1.388971	-1.39

Table 10. Measure of distribution entropy

Number	2	3	4	5	6	9	10	11	12	13	14
Measure	- 0.14*	- 1.18	- 1.65	- 1.37	- 3.52	- 3.92	- 3.64	- 3.26	- 3.97	- 3.86	- 3.75

Where * is the maximum value

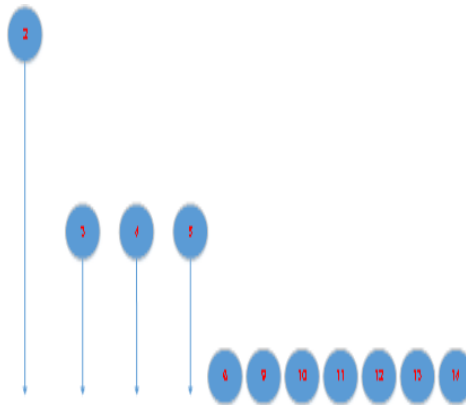


Figure 6. Sequence of distribution entropy

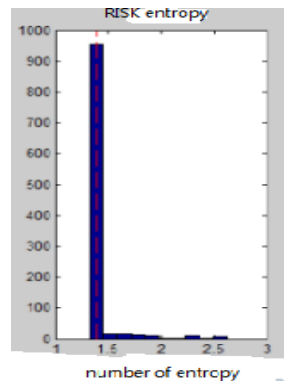


Figure 7. Sequence of risk entropy

4. Conclusion

In this paper, the mixed entropy measure method is proposed to analyze the fragility of the fault of IEEE14 nodes. Compared with the power flow entropy method

or the risk entropy method, the proposed method has the advantage that the sequence of distribution entropy can be quantized with the number of distribution entropy. On the other hand, the proposed method can achieve better solutions for the same computational effort. Further research work includes that a high performance method for the power network vulnerability analysis with large nodes.

Acknowledgments

This paper is supported by Natural Science Foundation of Fujian Province under grant (grant number 2016H6019, 2016J01267), in part by Scientific and Technological Projects of Fuzhou City (grant number 2016-G-53), in part by scientific research project of Xiamen City (grant number 3502Z20189033), in part by the Scientific Research Items of MJU [grant number MJY18003]

Reference

- Ardakani A. J., Bouffard F. (2013). Identification of umbrella constraints in DC-based security constrained optimal power flow. *IEEE Trans. Power Syst*, Vol. 28, No. 4, pp. 3924–3934. <http://doi.org/10.1109/TPWRS.2013.2271980>
- Barocio E., Regalado J., Cuevas E. (2017). Modified bio-inspired optimization algorithm with a centroid decision making approach for solving a multi-objective optimal power flow problem. *IET Generation Transmission & Distribution*, Vol. 11, No. 4, pp. 1012–1022. <http://doi.org/10.1049/iet-gtd.2016.1135>
- Bucha B., Janák J. (2014). A MATLAB-based graphical user interface program for computing functionals of the geopotential up to ultra-high degrees and orders. *Pergamon Press, Inc.* Vol. 56, pp. 186–196. <http://doi.org/10.1016/j.cageo.2013.03.012>
- Capitanescu F. (2011). Contingency filtering techniques for preventive security-constrained optimal power flow. *Elect. Power Syst. Res*, Vol. 81, No. 8, pp. 1731–1741. <http://doi.org/10.1109/TPWRS.2007.907528>
- Capitanescu F., Wehenkel L. (2012). Sensitivity-based approaches for handling discrete variables in optimal power flow computations. *IEEE Trans. Power Syst*, Vol. 25, No. 4, pp. 1780–1789. <http://doi.org/10.1109/TPWRS.2010.2044426>
- Carvalho L. D. M., Silva A. M. L. D., Miranda V. (2018). Security-constrained optimal power flow via cross-entropy method. *IEEE Transactions on Power Systems*, No. 99, pp. 1–1. <http://doi.org/10.1109/TPWRS.2018.2847766>
- Christopher B., Rua M. (2014). Maximum entropy estimates for risk-neutral probability measures with non-strictly-convex data. *Journal of Optimization Theory and Applications*, Vol. 161, No. 1, pp. 285–307. <http://doi.org/10.1007/s10957-013-0349-x>
- Fang R., Shang R., Wang Y. (2017). Identification of vulnerable lines in power grids with wind power integration based on a weighted entropy analysis method. *International Journal of Hydrogen Energy*, Vol. 42, No. 31. <http://doi.org/10.1016/j.ijhydene.2017.06.039>
- Green M., Pierre P. D., Derby K. (2003). Ground plane insulation failure in the first TPC superconducting coil. *IEEE Transactions on Magnetics*, Vol. 17, No. 5, pp. 1855–1859. <http://doi.org/10.1109/tmag.1981.1061311>

- Iacoboaiea O. C., Sayrac B., Jemaa S. B. (2016). On mobility parameter configurations that can lead to chained handovers. *IEEE Transactions on Communications*, Vol. 64, No. 12, pp. 5136-5148. <http://doi.org/10.1109/TCOMM.2016.2615613>
- Kazemdehdashti A., Mohammadi M., Seifi A. R. (2018). The generalized cross-entropy method in probabilistic optimal power flow. *IEEE Transactions on Power Systems*, No. 99, pp. 1-1. <http://doi.org/10.1109/TPWRS.2018.2816118>
- Marano-Marcolini A., Capitanescu F., Martinez-Ramos J., Wehenkel L. (2012). Exploiting the use of DC SCOPF approximation to improve iterative AC SCOPF algorithms. *IEEE Trans. Power Syst*, Vol. 27, No. 3, pp. 1459–1466. <http://doi.org/10.1109/tpwrs.2012.2186469>
- Momoh J. A. (2009). *Electric Power System Applications of Optimization*. Boca Raton, FL, USA: CRC Press.
- Monticelli A. J., Pereira M. V. P., Granville S. (1987). Security-constrained optimal power flow with post-contingency corrective rescheduling. *IEEE Trans. Power Syst*, Vol. 2, No. 1, pp. 175–182. <http://doi.org/10.1109/TPWRS.1987.4335095>
- Phan D., Kalagnanam J. (2012). Some efficient optimization methods for solving the security-constrained optimal power flow problem. *IEEE Trans. Power Syst*, Vol. 29, No. 2, pp. 836-872. <http://doi.org/10.1109/TPWRS.2013.2283175>
- Platbrood L., Capitanescu F., Merckx C., Crisciu H., Wehenkel L. (2014). A generic approach for solving nonlinear-discrete security-constrained optimal power flow problems in large-scale systems. *IEEE Trans. Power Syst*, Vol. 29, No. 3, pp. 1194–1203. <http://doi.org/10.1109/TPWRS.2013.2289990>
- Shahidehpour M., Yamin H., Li Z. (2002). *Market operations in Electric Power Systems: Forecasting, Scheduling, and Risk Management*. Hoboken, NJ, USA: Wiley-IEEE Press.
- Stott B., Alsac O., Monticelli A. J. (1987). Security analysis and optimization. *Proc. IEEE*, Vol. 75, No. 12, pp. 1623-1644. <http://doi.org/10.1109/PROC.1987.13931>
- Thomasian A., Blaum M. (2006). Mirrored disk organization reliability analysis. *IEEE Transactions on Computers*, Vol. 55, No. 12, pp. 1640-1644. <http://doi.org/10.1109/tc.2006.201>
- Wang Q., McCalley J. D., Tongxin Z., Litvinov E. (2013). A computational strategy to solve preventive risk-based security constrained OPF. *IEEE Trans. Power Syst*, Vol. 28, No. 2, pp. 1666-1675. <http://doi.org/10.1109/tpwrs.2012.2219080>
- Wang W. Q., Wang D., Singh V. P. (2018). Optimization of rainfall networks using information entropy and temporal variability analysis. *Journal of Hydrology*, No. 559. <http://doi.org/10.1016/j.jhydrol.2018.02.010>
- Wang Y., Shahidehpour M., Lai L. L. (2018). Resilience-constrained hourly unit commitment in electricity grids. *IEEE Transactions on Power Systems*, No. 99, pp. 1-1. <http://doi.org/10.1109/TPWRS.2018.2817929>
- Wood A. J., Wollenberg B. F., Sheble G. B. (2014). *Power Generation, Operation, and Control*. Hoboken, NJ, USA: Wiley.
- Zhu J. (2009). *Optimisation of Power System Operation*. Hoboken, NJ, +USA: Wiley-IEEE Press. <http://doi.org/10.3176/oil.2013.2S.01>